Regular Article

blood

LYMPHOID NEOPLASIA

An oxidative stress-based mechanism of doxorubicin cytotoxicity suggests new therapeutic strategies in ABC-DLBCL

Yun Mai,[1] J. Jessica Yu,[1] Boris Bartholdy,[1] Zijun Y. Xu-Monette,[2] Esther E. Knapp,[3,4] Fei Yuan,[1] Hongshan Chen,[1] B. Belinda Ding,[1] Zhihua Yao,[2] Bhaskar Das,[5] Yiyu Zou,[6] Ken He Young,[2] Samir Parekh,[1,6] and B. Hilda Ye[1]

[1]Department of Cell Biology, Albert Einstein College of Medicine and Montefiore Medical Center, Bronx, New York, NY; [2]Department of Hematopathology, The University of Texas MD Anderson Cancer Center, Houston, TX; [3]Department of Pediatrics, [4]The Children's Hospital at Montefiore, [5]Department of Nuclear Medicine, and [6]Department of Medicine, Albert Einstein College of Medicine and Montefiore Medical Center, Bronx, New York, NY

Key Points

- Dox causes DNA damage inefficiently in ABC-DLBCL because of preferential cytoplasmic localization.
- STAT3 promotes resistance to ROS-mediated Dox cytotoxicity by upregulating the expression of SOD2.

Diffuse large B-cell lymphomas (DLBCLs) contain 2 major molecular subtypes; namely, the germinal center B-cell-like (GCB) and the activated B-cell-like (ABC) DLBCLs. It is well documented that ABC-DLBCL cases have a significantly poorer survival response than GCB-DLBCLs in both the CHOP (cyclophosphamide, vincristine, doxorubicin, and prednisone) and the rituximab (R)-CHOP eras. However, the underlying cause of this subtype disparity is poorly understood. Nevertheless, these clinical observations raise the possibility for an ABC-DLBCL–specific resistance mechanism that is directed toward 1 of the CHOP components and is inadequately addressed by rituximab. Here, we report that the main cytotoxic ingredient in CHOP, doxorubicin (Dox), has subtype-specific mechanisms of cytotoxicity in DLBCLs resulting from differences in the subcellular distribution pattern. Specifically, in cell line models of ABC-DLBCL, Dox is often enriched in the cytoplasm away from the nuclear DNA. As a result, Dox-induced cytotoxicity in ABC-DLBCLs is often dependent on oxidative stress, rather than DNA damage response. These findings are corroborated by gene signature analysis, which demonstrates that basal oxidative stress status predicts treatment outcome among patients with ABC-DLBCL, but not patients with GCB-DLBCL. In terms of redox-related resistance mechanism, our results suggest that STAT3 confers Dox resistance in ABC-DLBCLs by reinforcing an antioxidant program featuring upregulation of the *SOD2* gene. Furthermore, a small-molecule STAT3 inhibitor synergizes with CHOP to trigger oxidative stress and kill ABC-DLBCL cells in preclinical models. These results provide a mechanistic basis for development of novel therapies that target either STAT3 or redox homeostasis to improve treatment outcomes for ABC-DLBCLs. (*Blood*. 2016;128(24):2797-2807)

Introduction

Diffuse large B-cell lymphoma (DLBCL) is a common B-cell malignancy resulting from the transformation of germinal center (GC) B cells.[1] DLBCL has 2 major molecular subtypes, GC B-cell-like (GCB) and activated B-cell-like (ABC), which differ in their immunophenotype, tumor biology, and clinical course.[2,3] Many biological characteristics that distinguish these 2 subtypes are dictated by distinct somatic mutations in these tumor cells.[1,4,5] For example, although GCB-DLBCLs abundantly express the GC master regulator BCL6, but lack NF-κB or STAT3 activation, ABC-DLBCLs express somewhat lower levels of BCL6, but exhibit constitutively activated NF-κB and STAT3 as the result of genetic alterations in upstream signaling molecules in the B-cell receptor and Toll-like receptor signaling pathways.[6-8] Both NF-κB and STAT3 regulate a diverse array of cellular pathways and are required for optimal growth and survival of lymphoma cells,[9-11] yet only STAT3, not NF-κB, has been implicated as a poor prognostic factor in DLBCL.[12]

Previously, when managed with the chemotherapy regimen CHOP (cyclophosphamide, vincristine, doxorubicin [Dox], and prednisone), the 5-year overall survival (OS) rates for patients with GCB-DLBCL and ABC-DLBCL were 46% and 32%, respectively.[2] The addition of the anti-CD20 monoclonal antibody rituximab to the CHOP backbone (R-CHOP) has markedly improved the survival outcomes of both subgroups, resulting in 5-year OS rates of ~80% and 50% for GCB-DLBCL and ABC-DLBCL, respectively.[2,13] Yet a significant survival disparity persists between these 2 subgroups, and the underlying biological basis is poorly understood. Although the approach of combining targeted agents with front-line treatment has received significant interest and showed promise in early clinical trials,[14,15] we believe additional therapeutic opportunities may arise with a better understanding of the ABC-DLBCL-associated mechanism of resistance to frontline treatment. In this regard, recent evidence suggests rituximab may not significantly alter survival outcomes for patients with relapsed/refractory DLBCL, which are often of the ABC-DLBCL subtype.[16] Such clinical observations raise the possibility for an ABC-DLBCL-specific resistance mechanism that is directed toward CHOP components and is inadequately addressed by rituximab. The notion of a subtype-specific resistance mechanism is also supported by reports that p53 mutations and constitutively activated STAT3 selectively

Submitted 15 March 2016; accepted 3 October 2016. Prepublished online as *Blood* First Edition paper, 13 October 2016; DOI 10.1182/blood-2016-03-705814.

The online version of this article contains a data supplement.

The publication costs of this article were defrayed in part by page charge payment. Therefore, and solely to indicate this fact, this article is hereby marked "advertisement" in accordance with 18 USC section 1734.

predict poor prognosis in the GCB- and ABC-DLBCL subgroups, respectively.[12,17]

Among the 3 anticancer drugs in CHOP, Dox is arguably the most important cytotoxic ingredient. Its major anticancer effects occur through the inhibition of topoisomerase II and generation of DNA double-strand breaks.[18,19] In this scenario, Dox rapidly activates the DNA damage response (DDR) pathway in cancer cells, leading to p53 activation and apoptosis.[20,21] The second cytotoxic mechanism of Dox, often discussed in the context of cardiotoxicity but also occurring in Dox-treated cancer cells, is oxidative stress caused by reactive oxygen species (ROS) originating from damaged mitochondria.[22,23] Yet the relative contribution of ROS to overall cytotoxicity and clinical outcome is rarely compared directly with the desired on-target effects; for example, DDR. Here, we demonstrate that Dox induces cytotoxicity in DLBCLs through subtype-specific mechanisms and that by promoting a cellular antioxidant program, activated STAT3 specifically antagonizes Dox-triggered oxidative cell death, which is the primary mechanism of cytotoxicity in ABC-DLBCL cells. We also show that a small molecule STAT3 inhibitor, CPA-7, can synergize with Dox-containing therapy in ABC-DLBCL preclinical models.

Methods

Cell culture and transient transfection

Cell lines were cultured in RPMI 1640 medium supplemented with 10% fetal bovine serum or, for the OCI-Ly series of cell lines, Iscove modified Dulbecco medium supplemented with 10% fetal bovine serum, with the exception of Ly10, which was cultured in Iscove modified Dulbecco medium plus 20% human plasma. Transient transfection procedure has been previously described.[9]

In vitro cytotoxicity assays and ROS measurement

Resazurin (R&D Systems)-based viability assays were used to determine the 50% inhibitory concentration (IC_{50}) values of Dox and H_2O_2 (Sigma-Aldrich) after exposing cells to various concentrations of the reagents for 48 and 8 hours, respectively. Unless specified, the cell line–specific Dox IC_{50} concentrations (supplemental Table 1, available on the *Blood* Web site) were used in all experiments in this study. The combination index (CI) and isobologram plots for CPA-7 and Dox interaction were generated with the Calcusyn software (Biosoft) on the basis of the method of Chou and Talalay.[24] With this method, the CI represents the degrees of synergism, with the smallest values indicating the most synergy. CI values less than 0.8 indicate synergy. Specifically, those values from 0.8 to 1.2 indicate an additive effect, and those more than 1.2 indicate antagonism. Mitochondrial superoxide was detected by MitoSox Red (Invitrogen) staining, and the results were shown as mean fluorescent intensity. Standard Annexin V+PI staining was used to quantify apoptotic and total viable cell fractions.

Quantitative RT-PCR and immunoblotting

Immunoblotting and quantitative reverse transcription polymerase chain reaction (qRT-PCR) were performed using standard techniques, as previously described.[25] To detect H2A and γH2AX, which bind DNA tightly, cells were lysed in Laemmli buffer (60 mM Tris·Cl at pH 6.8, 4% SDS, 10% glycerol) and then sonicated in an ice-cold water bath for 40 × 5 seconds, with 5-second intervals between the cycles, using a Diagenode Bioruptor at high power setting. Primary antibodies used for Immunoblot analysis were purchased from Santa Cruz Biotechnology for STAT3 (sc-482), GAPDH (sc-25778), Mcl-1 (sc-819), JunB (sc-8051), and c-Myc (sc-40); from Cell Signaling Technology for PY-STAT3 (#9131), PS-STAT3 (#9123), P-CHK2 (#2661), CHK2 (#2662), P-p53 (#9284), p53 (#2524), phosphor-histone H2AX (#2577), and H2A; from GeneTex for ATM (GTX70103); and from R&D systems for P-ATM (AF1655).

Quantitative chromatin immunoprecipitation

Locus-specific quantitative chromatin immunoprecipitation (qChIP) was performed as previously described.[25] The control rabbit immunoglobulin G and anti-STAT3 (sc-482) polyclonal antibodies were from Santa Cruz Biotechnology. The *SOD2* primers used for qPCR measurement of the recovered genomic DNA are GTCCCAGCCTGAATTTCC (forward) and CTAGGCTTC CGGTAAGTG (reverse).

Imaging of subcellular Dox distribution; CHOP and CPA-7 treatment of animals; prognostic analysis based on an oxidative stress gene expression signature

The detailed procedure is described in the supplemental Methods.

Statistical analysis

Unpaired 2-tailed Student *t* test and linear regression analysis were performed where appropriate, using Excel 2010. The Kaplan-Meier method was used to estimate the survival distributions, with the log-rank test performed to compare the survival curves. The survival analysis was performed using the GraphPad Prism 6 software. Statistical significance was set at a level of $P < .05$.

Results

DDR plays a major role in Dox-triggered cytotoxicity in GCB-DLBCL, but not ABC-DLBCL, cell lines

Dox is a substrate of the drug transporter P-glycoprotein, which is variably expressed in primary DLBCLs.[26] As such, a given concentration of Dox may result in marked variations in its intracellular concentration in cultured DLBCL cells, therefore complicating our investigation because the biological actions of Dox are dose-dependent.[27] To circumvent this issue and focus on the primary mode of cytotoxicity, we first determined the Dox IC_{50} values for all DLBCL cell lines used in this study (supplemental Table 1) and applied these individually determined doses throughout this study unless otherwise indicated.

To evaluate DDR response to Dox, we monitored 4 DDR markers in 5 GCB and 6 ABC-DLBCL cell lines for 24 hours after Dox treatment. In all GCB cell lines tested, robust DDR activation was observed, as evidenced by rapid increase in phospho-Ser1981-ATM (P-ATM), phospho-Thr68-CHK2 (P-CHK2), and phospho-Ser139-H2AX (γH2AX; Figure 1A; supplemental Figure 1). The p53 response was more variable, with the increase in total p53 and phospho-Ser15-p53 (P-p53) being strong and progressive in Val and Ly1 and weak and transient in SUDHL5. Neither total p53 nor P-p53 could be detected in Karpas-422 and Pfeiffer, likely because of extremely low p53 mRNA expression.[28] In the 6 ABC cell lines examined, however, moderate to strong DDR was observed only in U2932 and SUDHL2 (supplemental Figure 1). In HBL1 cells (supplemental Figure 1), despite normal ATM activation, the DDR signal was not transduced to the ATM substrates CHK2 and H2AX. In the other 3 ABC-DLBCL cell lines, Riva, Ly3 (Figure 1A), and Ly10 cells (supplemental Figure 1), Dox completely failed to activate ATM, CHK2, and H2AX. Similar results were obtained when γH2AX signals were measured by flow cytometry (not shown). Of note, strong P-p53 signals were occasionally observed in the absence of CHK2 activation in ABC-DLBCL cell lines, for example, Riva (Figure 1A) and HBL1 (supplemental Figure 1), possibly as the result of cellular stress other than DDR.[29] To exclude the possibility that the DDR pathway in ABC-DLBCL cell lines is functionally compromised, we examined the status of DDR

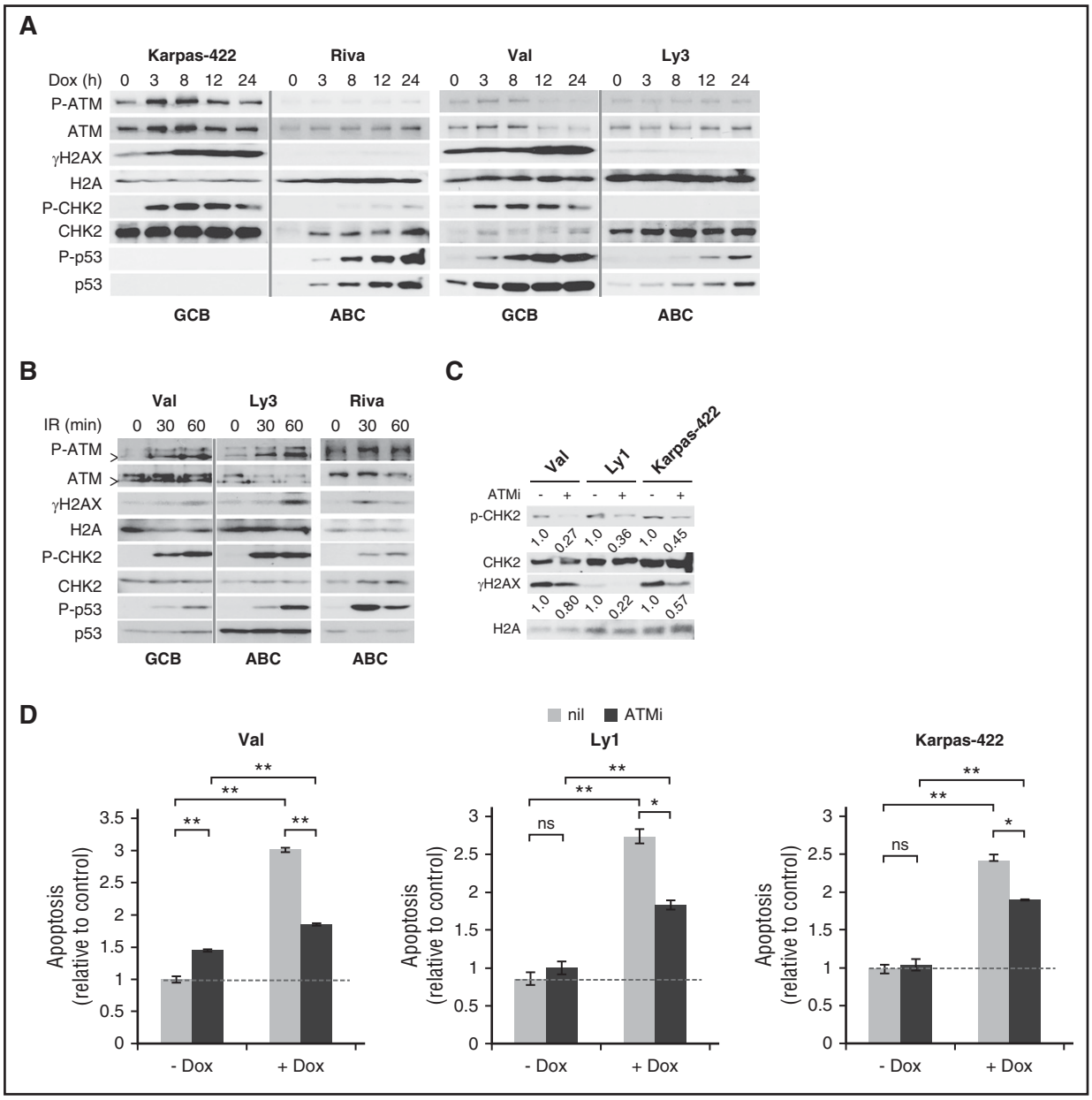

Figure 1. DDR plays a major role in Dox-triggered cytotoxicity in GCB-DLBCL, but not ABC-DLBCL, cell lines. (A) Immunoblot analysis of DDR markers during a 24-hour Dox treatment course in cell lines representing the GCB (Val and Karpas-422) and ABC (Ly3 and Riva) subtypes. (B) Immunoblot analysis of DDR markers in response to ionizing radiation (IR; 1.4 Gy/min) at the indicated points in 1 representative GCB (Val) and 2 representative ABC (Ly3 and Riva) cell lines. In A and B, vertical gray lines demarcate samples from different cell lines that were loaded on the same gel. >, a shorter ATM protein that is likely a degradation product of ATM.[56] CHK2 and H2AX phosphorylation (C) and apoptosis (D) after a 20-hour Dox treatment with or without a 1-hour preincubation with the ATM inhibitor (ATMi), KU-55933. Results shown in the bar graphs are mean ± SD and are representative of 2 independent experiments. Two-tailed Student *t* test was used for pairwise comparison as indicated. $^{*}P < .05$; $^{**}P < .01$; ns, not significant. nil, vehicle control. Dotted horizontal lines mark the basal level of apoptosis in untreated samples.

after ionizing irradiation (IR) (Figure 1B; supplemental Figure 2). With the exception of P-CHK2 in HBL1, DDR activation in the 6 ABC cell lines was fairly comparable to 2 representative GCB lines, Val and SUDHL6, indicating that the ABC-DLBCL cell lines have a functionally intact DDR pathway, and thus inefficient DDR activation by Dox is most likely a result of its failure to generate DNA damage, rather than defective DDR signaling.

We also evaluated the functional importance of DDR in Dox-treated GCB-DLBCL cells. Three GCB-DLBCL cell lines were exposed to Dox for 20 hours, either with or without a pretreatment with the ATM inhibitor, KU-55933 (ATMi). The effect of ATMi on DDR response and apoptosis was then evaluated. As shown in Figure 1C, inhibiting ATM reduced Dox-induced P-CHK2/γH2AX signals by 73%/20%, 64%/78%, and 55%/43% in Val, Ly1, and Karpass-422 cells, respectively. Dox-induced apoptosis was similarly reduced in these cell lines (58% in Val; 49% in Ly1, and 37% in Karpass-422; Figure 1D). These results indicate that DDR is a major mechanism of Dox-triggered cell death in GCB-DLBCL cells, at least during the early phase of drug exposure. However, other mechanisms of cell death may also contribute to the overall cytotoxicity.

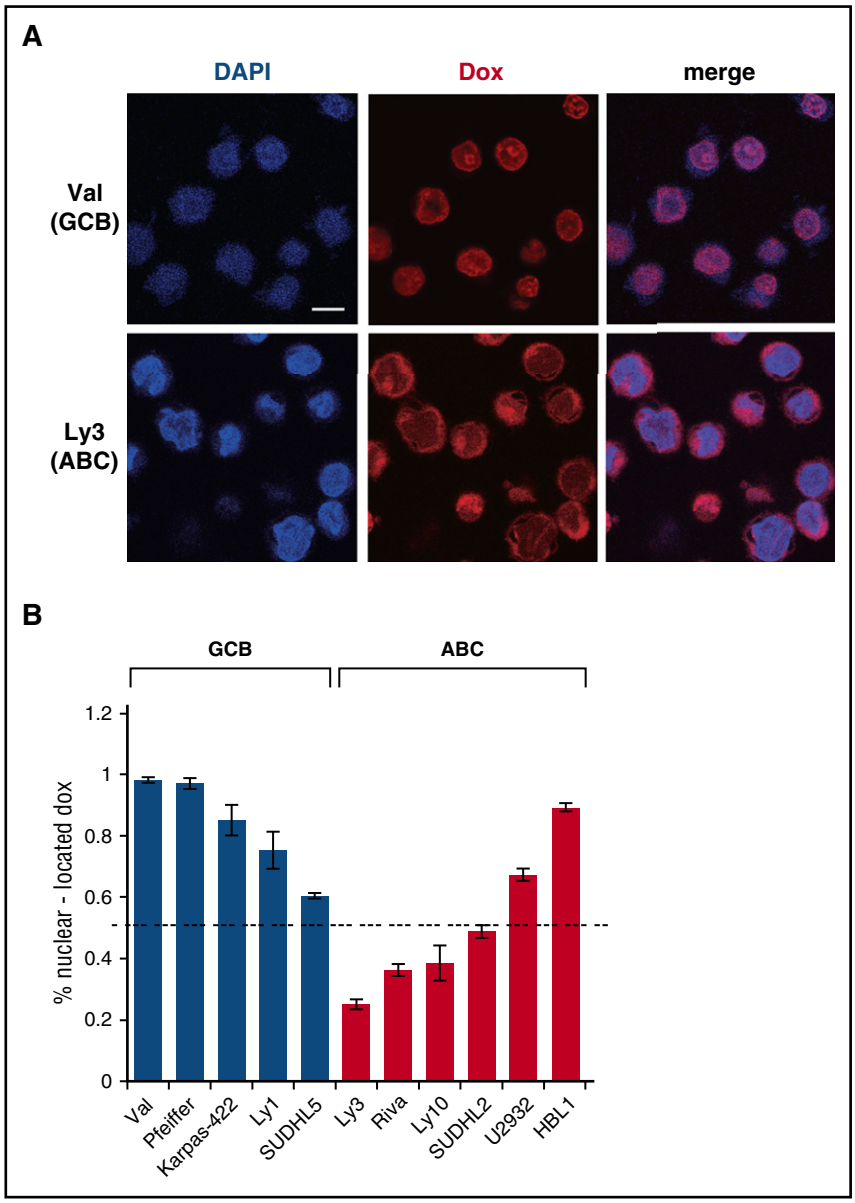

Figure 2. Dox is often enriched in the cytoplasm in ABC-DLBCL cell lines. (A) Subcellular distribution of Dox in representative GCB (Val) and ABC (Ly3) cell lines, as assessed by confocal microscopy after treating cells with IC_{50} concentrations of Dox for 24 hours. Scale bar, 10 μM. Quantification of the confocal microscopy data from 4 GCB and 5 ABC cell lines is summarized in (B). Error bars indicate SD from measurements of multiple cells (see supplemental Methods for details). Dotted horizontal line marks the 50% level of nuclear Dox enrichment.

Dox is often excluded from the nucleus in the ABC-DLBCL cell lines

To investigate the cause of inefficient DDR activation by Dox in ABC-DLBCL cells, we examined subcellular distribution of Dox, using confocal microscopy (Figure 2A-B). These confocal analyses showed that in all 5 GCB-DLBCL cell lines, at least 60% of the Dox signals were concentrated in the nucleus. Among these, SUDHL5 had the lowest amount of nuclear Dox (60%), correlating with a weaker DDR response relative to other GCB lines (supplemental Figure 1). Among the 6 ABC-DLBCL cell lines tested, only 2 had 60% or more Dox signals in the nucleus. The 3 cell lines showing the least concentration of nuclear Dox (Ly3, Ly10, and Riva) were also the ones that were most resistant to Dox-induced DDR (Figure 1A; supplemental Figure 1). In comparison, the 3 cell lines showing 50% to 90% nuclear Dox signals had moderate (SUDHL2 and HBL1) to strong (U2932) DDR activation (supplemental Figure 1). Therefore, inefficient DDR activation by Dox in ABC-DLBCL cells is likely caused by inadequate nuclear accumulation of Dox.

ROS is a major contributor to Dox-induced cell death in ABC-DLBCL cells

Given the paucity of DDR in many ABC-DLBCL cell lines treated with IC_{50} concentrations of Dox, we subsequently evaluated the role of ROS. Mitochondrial superoxide (O_2^-) is referred to as ROS in the following experiments because changes in this ROS species correlated more closely with cell survival than hydrogen peroxide (not shown). Ly3 and Ly10 cells treated with Dox for more than 16 hours showed progressive ROS accumulation, which was mirrored by steady decline in cell viability (Figure 3A). When cells were pretreated with antioxidants (*N*-acetyl-cysteine and vitamin C), to antagonize Dox-induced ROS, Dox-triggered increase in cell death was also substantially reduced, often to pretreatment levels (Figure 3B). In the case of vitamin C–treated Ly10 cells, a small reduction in ROS led to a substantial restoration of viability, possibly suggesting a threshold effect in ROS-induced cell signaling and cell death. However, in Riva cells, attenuation of Dox-induced ROS increase by antioxidants did not restore the total number of viable cells, possibly because Dox mainly

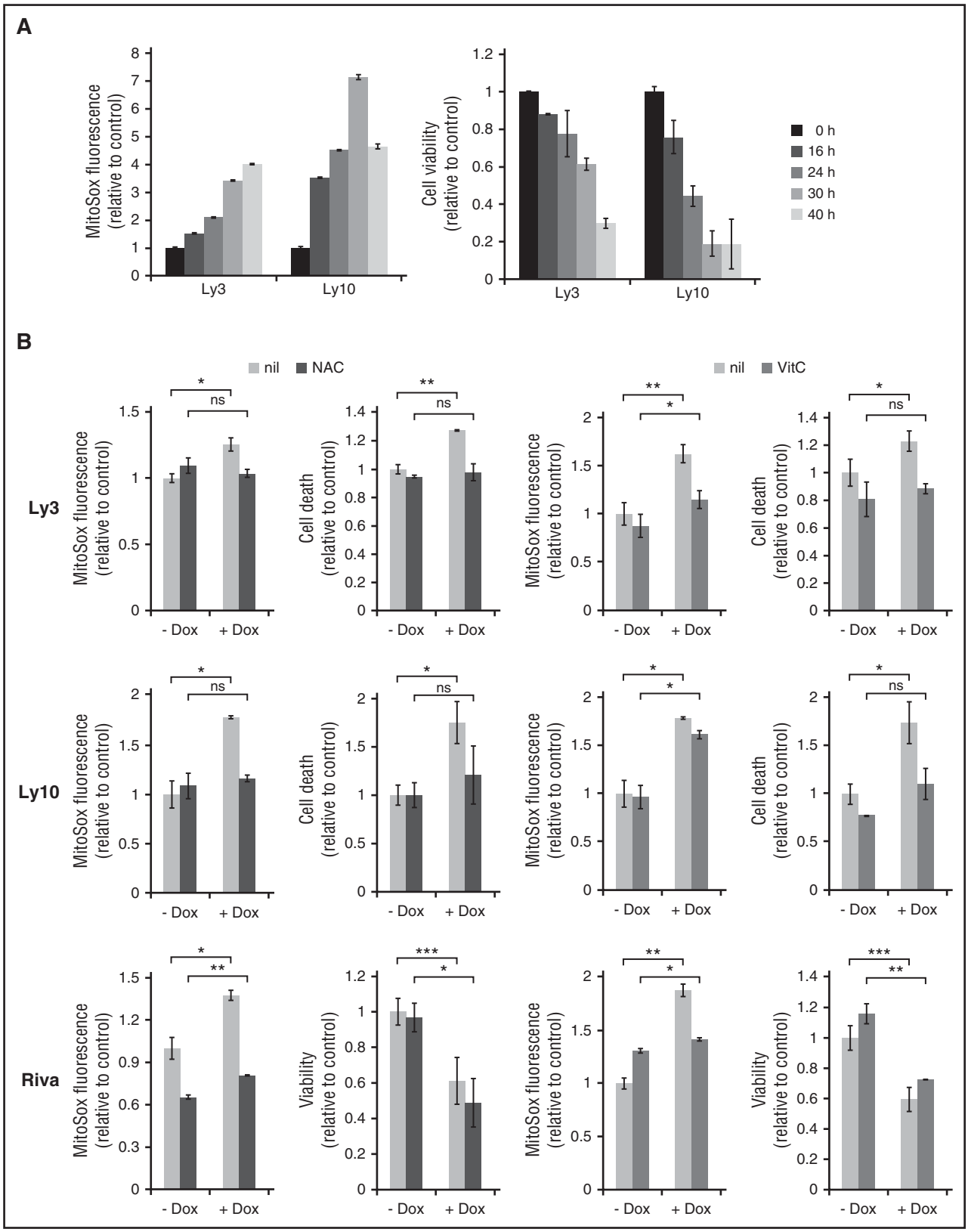

Figure 3. ROS is a major cause of Dox-triggered cell death in ABC-DLBCL cell lines. (A) Changes in cellular ROS levels and viability during a 40-hour Dox treatment. Data from 2 representative ABC-DLBCL cell lines, Ly3 and Ly10, are shown. Viable fraction is defined as Annexin V-neg/Propidium Iodide (PI)-neg cells. (B) The effect of antioxidants on Dox-induced ROS accumulation and cell viability change. Ly3, Ly10, and Riva cells were pretreated with either *N*-acetyl-cysteine or vitamin C for 1 h before exposing to Dox for 18 hours. ROS measurement was based on mean fluorescent intensity of MitoSox staining, followed by flow cytometry. For Ly3 and Ly10, cell death was defined as the proportion of all Annexin V+ cells. For Riva, viable cells were enumerated based on Trypan blue exclusion. Results shown are mean ± SD and are representative of 2 independent experiments. Two-tailed Student *t* test was used for pairwise comparison, as indicated. $^{*}P < .05$; $^{**}P < .01$; ns, not significant. nil, vehicle control.

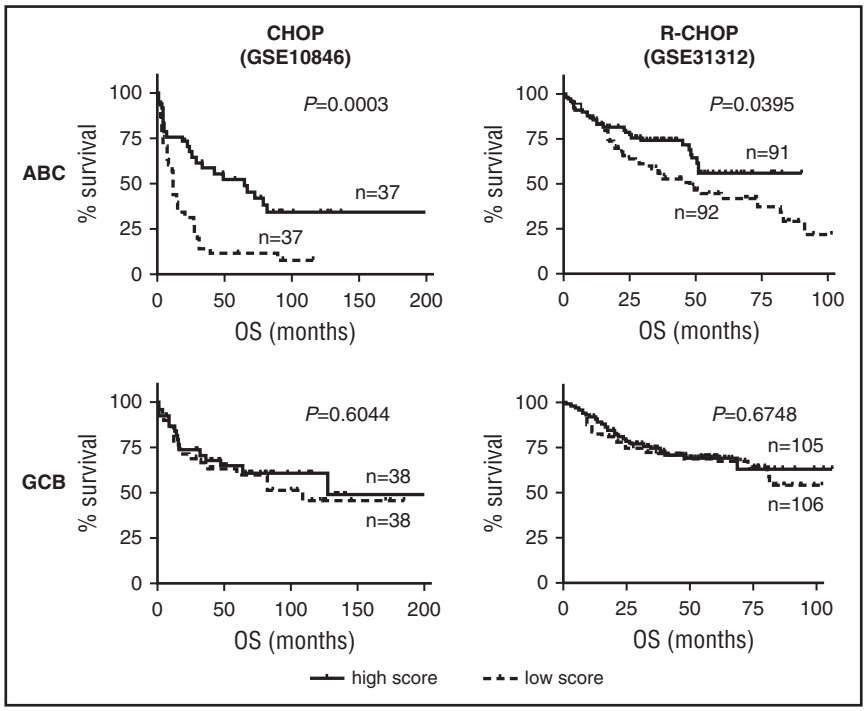

Figure 4. Basal oxidative stress status is predictive of treatment outcome among patients with ABC-DLBCL, but not GCB-DLBCL. OS response of patients with DLBCL according to ABC/GCB subtype status and expression level of a cellular oxidative stress gene signature. ABC-specific prognostic significance is observed in a CHOP cohort (GSE10846) and an R-CHOP cohort (GSE31312). *P* values of log-rank test between patients with a low (<50th percentile) and high (>50th percentile) signature score are indicated.

reduced cell proliferation instead of causing cell death in this cell line (Figure 3B). We conclude from these results that elevated ROS is a major cause of Dox-triggered cell death in ABC-DLBCL cells. However, Dox-induced cytostatic effect may be less dependent on ROS.

Basal oxidative stress status predicts treatment outcome among patients with ABC-DLBCL, but not GCB-DLBCL

The antioxidant experiments suggested that, at least in the cell line models of ABC-DLBCL, the pretreatment redox state could significantly influence Dox-induced ROS accumulation and cell survival. To test the validity of this notion in a clinical setting, we evaluated the prognostic significance of a gene expression signature composed of 16 experimentally validated oxidative stress pathway genes. Survival analysis was performed using previously published CHOP and R-CHOP cohorts[30] while stratifying patients into the ABC/GCB subtypes. Among the CHOP-treated patients with ABC-DLBCL, this oxidative stress signature had significant prognostic value ($P = .0003$), with 5-year OS rates of 52% and 11% for the high- and low-expressing subgroups, respectively. Yet no prognostic significance could be detected for the CHOP-treated GCB-DLBCL subgroup ($P = .604$) (Figure 4A). A similar, ABC-specific prognostic association was detected in an R-CHOP cohort ($P = .0395$; supplemental Figure 5B). Again, for the GCB subgroup of this cohort, this prognostic association was absent ($P = .6748$). To further confirm the subtype-specific role of cellular redox control in chemotherapy response, we measured the antioxidant capacity of a series of DLBCL cell lines, using the H_2O_2 toxicity test. We found a strong and direct correlation between IC_{50} values for H_2O_2 and Dox among the 9 ABC cell lines, and yet this relationship was absent among the 9 GCB cell lines (supplemental Figure 5C). When combined, these results indicate that the cellular antioxidant defense systems were selectively engaged when ABC-DLBCLs, but not GCB-DLBCLs, were treated with Dox-containing therapies; furthermore, ABC-DLBCL tumors with extensive preexisting redox adaptation responded to frontline treatment better, possibly because of their limited capacity to eradicate additional chemo-induced ROS.[31]

STAT3 confers chemoresistance to ABC-DLBCL cells by promoting a cellular antioxidant program

We have previously reported that STAT3 activation is a poor prognosticator among ABC-DLBCLs but has no prognostic effect among GCB-DLBCLs.[12] As such, we designed experiments to address the role of STAT3 in Dox-triggered cytotoxicity in ABC-DLBCLs. We first examined the possibility that activated STAT3 is casually involved in the cytoplasmic localization of Dox, and hence the weak DDR response in Dox-treated cells. However, STAT3 silencing did not potentiate DDR activation in ABC-DLBCL cell lines (supplemental Figure 6), indicating STAT3 is not responsible for the lack of a strong DDR response to Dox. In contrast, we observed that Dox treatment led to rapid and progressive increase in PY-STAT3 levels in multiple cell lines during the first 12 hours (Figure 5A). However, this increase dropped sharply at 24 hours, concurrent with marked accumulation of ROS (Figure 3A), suggesting a possibility that STAT3 is redox responsive in ABC-DLBCL cells and plays an active role in the cellular antioxidant defense. To experimentally test this possibility, we used siRNA to knock down the endogenous STAT3 in Ly3 and SuDHL2 cells. As shown in Figure 5B, STAT3 silencing modestly increased ROS on its own and significantly augmented Dox-induced ROS accumulation. When cell viability was measured, combining STAT3 silencing and Dox treatment appeared to have either additive (Ly3) or synergistic (SUDHL2) effects (Figure 5B). These results showed that STAT3 plays an antioxidant role in ABC-DLBCLs.

Because STAT3 exerts its biological functions mostly as a transcription factor, we moved to identify STAT3 target genes that can mediate its antioxidant function. First, we analyzed genomewide gene expression changes after STAT3 siRNA treatment in 4 ABC-DLBCL cell lines.[12] Among the top-ranked genes positively regulated by STAT3 was SOD2 (mitochondria superoxide dismutase). In independent STAT3 silencing experiments, we confirmed that STAT3 is a

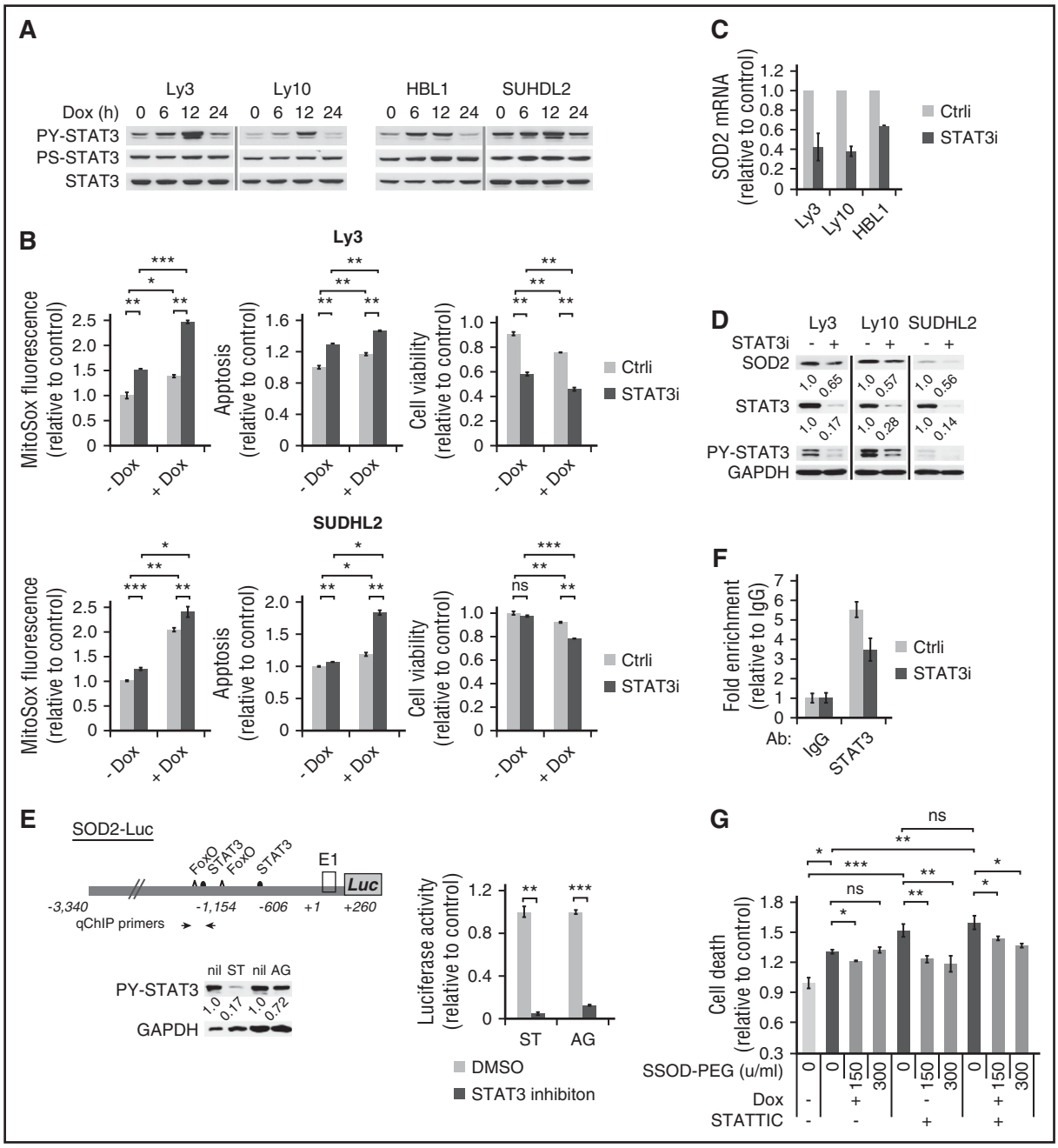

Figure 5. STAT3 confers chemoresistance to ABC-DLBCL cells by promoting a cellular antioxidant program. (A) Immunoblot analysis of PY705-STAT3 and PS727-STAT3 during a 24-hour Dox treatment course of 4 ABC-DLBCL cell lines. (B) The effect of STAT3 silencing on basal and Dox-induced ROS and cell viability change. Results from Ly3 and SUDHL2 cells were shown. ROS and cell viability measurements were made as in Figure 3. Cell viability was defined as the fraction of Annexin-neg/PI-neg cells. Forty-eight hours after transfection with either control (Ctrli) or STAT3-specific siRNA (STAT3i) oligos, changes in *SOD2* mRNA (C) and protein (D) were examined by qPCR and immunoblot, respectively. (E) Luciferase reporter assay measuring the effects of inhibitors to STAT3 (10 μM STATTIC; ST) and Jak (20 μM AG490; AG) on the activity of a luciferase construct driven by the 3.6-kb human *SOD2* promoter. SUDHL2 cells were used in transient transfections. (F) qChIP analysis was performed to measure in vivo binding of STAT3 to the *SOD2* promoter region in Ly3 cells that were transfected with either Ctrli or STAT3i oligos. Signals enriched by STAT3 Abs were normalized to that from the control rabbit IgG. Results shown in B, C, and E are mean ± SD and representative of 2 independent experiments. $^*P < .05$; $^{**}P < .01$; $^{***}P < .001$, based on 2-tailed Student *t* test. (G) SOD-PEG can attenuate cell death associated with STAT3 inactivation. Ly 3 cells with or without STATTIC pretreatment were exposed to Dox. At 4 and 19 hours into the Dox treatment, aliquots of the samples were treated with SOD-PEG at 75 or 150 U/mL. Cell death was defined as the proportion of all Annexin V+ cells at 24 hours after Dox exposure.

positive regulator of SOD2 expression at both the mRNA (Figure 5C) and protein levels (Figure 5D). In addition, the activity of a *SOD2* luciferase reporter containing 2 STAT3 sites[32] could be markedly suppressed by either the Jak inhibitor AG490 or the STAT3 inhibitor STATTIC (Figure 5E). Additional evidence supporting *SOD2* as a direct STAT3 target gene comes from ChIP experiments, which showed STAT3 occupancy of the endogenous *SOD2* promoter region (Figure 5F). In a complementary overexpression approach, we found that HBL1 cells forced to express the constitutively activated STAT3C had more SOD2 protein and acquired enhanced resistance against both Dox and H_2O_2 (supplemental Figure 7). Most important, SOD-PEG partially but significantly rescued the viability of cells exposed to either

STATTIC or Dox/STATTIC combination (Figure 5G), suggesting STAT3 promoted cell survival at least in part by enhancing superoxide clearance capability. Taken together, these findings demonstrate that STAT3 actively confers resistance to Dox-induced cytotoxicity in ABC-DLBCL cells by promoting antioxidant defense, at least in part, through upregulating SOD2.

A small molecule STAT3 inhibitor synergizes with Dox to kill ABC-DLBCL cells in vitro and in vivo

A direct and causal role of STAT3 in Dox resistance suggests a therapeutic opportunity based on STAT3 targeting. To test this concept, we turned to the platinum IV compound, CPA-7. CPA-7 has been widely used in oncology and immunology studies as a small molecule STAT3 inhibitor,[33-36] with its STAT3-inhibitory activity attributed to its ability to inhibit DNA binding of STAT3, but not STAT5.[34] We have exposed 14 DLBCL cell lines to increasing concentrations of CPA-7. In Figure 6A, the resistant group comprises 6 GCB cell lines, a PY-STAT3-negative ABC line Riva (supplemental Figure 8A), and a PY-STAT3-positive ABC line SUDHL2, where the endogenous PY-STAT3 is resistant to CPA-7 treatment of unknown reason (supplemental Figure 8B). The sensitive group contains 5 ABC-DLBCL cell lines and a GCB cell line SUDHL5, which has low levels of endogenous PY-STAT3 sensitive to CPA-7 (supplemental Figure 8B). These results indicate that the effect of CPA-7 on cell viability is contingent on its ability to decrease PY-STAT3. When CPA-7 was used at 5 μM, a notable decrease in PY-STAT3, c-Myc, and cyclin D2 was observed at 16 hours without degradation of MCL-1 (Figure 6B). When cells were treated with 2 μM CPA-7 for 16 hours, only a slight reduction in c-Myc was detected without any change in poly(ADP-ribose) polymerase 1. These results suggest that changes in PY-STAT3 and its downstream effectors occur early during CPA-7 treatment, and likely contributed to the cytotoxicity observed at later times, such as 24 hours. Next, we examined cellular changes after CPA-7-mediated STAT3 inhibition in combination with Dox. Treating Ly3 cells with 0.3 μM CPA-7 and the IC_{50} dose of Dox resulted in additive effects in ROS accumulation (Figure 6C, left). Although at this concentration, CPA-7 did not cause cell death on its own, it enhanced Dox-induced cytotoxicity. In HBL1 cells, combining CPA-7 and Dox produced additive effects in both ROS accumulation and cell death (Figure 6C, right).

Synergistic interactions between these 2 drugs was then evaluated using the isobologram method.[24] In Ly3 cells, moderate synergy (CI = 0.3-0.7) could be achieved with 3 to 8 nM Dox and 0.04 to 0.5 μM CPA-7. In Ly10 cells, very strong synergy (CI $<$ 0.2) could be achieved with 1 to 5 nM Dox and 0.1 to 0.2 μM CPA-7 (Figure 6D). Finally, we tested interaction between CPA-7 and CHOP therapy in ABC-DLBCL xenograft models (Figure 6E-F). At 3.5 mg/kg, CPA-7 alone did not show any antilymphoma activity against established Ly3 tumors. However, it markedly potentiated the therapeutic activity of CHOP, as evidenced by significantly reduced tumor burden in the group receiving CHOP+CPA-7 relative to the CHOP treatment group (Figure 6E). Although the treatment was administered only once, 3 of the 6 mice in the CHOP+CPA-7 group, but none of the animals in the other treatment groups, showed complete tumor regression that lasted for 5 to 7 days (not shown). In the case of Ly10 xenograft, although CPA-7 and CHOP each showed significant therapeutic activity relative to the vehicle-treated control group, the combination resulted in substantially prolonged duration of response from 8 (CAP-7 only) to 10 (CHOP only) days to 28 days (Figure 6F). Combined with the results obtained using the STAT3 siRNA approach (Figure 5), these findings in preclinical models strongly support the notion that targeting STAT3 can sensitize ABC-DLBCLs to Dox-containing therapy.

Discussion

In recent years, in-depth characterization of the DLBCL mutational landscape has led to much improved understanding of pathogenesis and has guided development of molecularly targeted therapies based on subtype-specific oncogenic pathways. Nevertheless, because targeted agents for DLBCL are often combined with the frontline therapy in early trials, and combinatorial therapies are a favored approach to combat resistance to molecularly targeted treatment,[37,38] resistance mechanisms directed toward the backbone of CHOP and R-CHOP will likely remain relevant for clinical practice in the foreseeable future. Our findings in this study demonstrate that the key cytotoxic ingredient in CHOP and R-CHOP, Dox, triggers robust DDR in the more therapy-responsive GCB-DLBCLs, yet often relies on ROS to kill therapy-refractory ABC-DLBCLs. This conclusion is supported by experimental results obtained from cell-line models and prognostic analysis of patients with DLBCL. Furthermore, because STAT3 is selectively activated in ABC-DLBCL cells, where it can promote antioxidant defense, the Dox–ROS–cell death cascade may operate rather inefficiently, with its cell death outcome strongly opposed by STAT3, but less so by p53 (Figure 6G). These novel insights also explain why the prognostic significance of activated STAT3 and mutated p53 is restricted to the ABC and GCB subtypes, respectively.[12,17]

The most unexpected finding in this study is the poor nuclear accessibility of Dox in many ABC-DLBCL cells. Although all GCB-DLBCL cell lines retained at least 60% of Dox in the nucleus, 4 of the 6 ABC cell lines examined fell below this benchmark. In cardiomyocytes, selective enrichment of Dox in mitochondria is attributed to the enormous mitochondria mass and the fact that Dox has an extraordinarily high affinity for cardiolipin, a lipid component highly enriched in the mitochondria inner membrane.[39] In solid tumors, one mechanism of chemoresistance is drug accumulation in discrete cytoplasmic organelles and sequestration away from the nucleus.[40,41] In drug-resistant breast cancer cells, this has been attributed to aberrant organelle acidification, which turns the organelles into traps for partially hydrophobic and weakly basic molecules such as Dox.[42] The exact cause of cytoplasmic Dox enrichment in ABC-DLBCL cells is currently unknown and is a subject for future research. Yet, because our cell line models carry a heterogeneous array of somatic mutations found in primary DLBCL samples,[43] the underlying cause is more likely related to the general cell physiology characteristics of ABC-DLBCLs, rather than any particular genetic mutations.

Our work here also demonstrates that STAT3 plays an antioxidant role in ABC-DLBCL cells by responding to Dox-induced oxidative stress and directly upregulating SOD2. This conclusion is based on several lines of evidence, including siRNA-mediated STAT3 silencing, expression of STAT3C in stable lines, and direct involvement of Jak/STAT3 in *SOD2* transcription regulation. Although a multitude of cellular functions has been attributed to constitutively activated STAT3 in cancer,[44,45] a direct role of STAT3 in antioxidant defense has not been documented. In fact, published literature contains many conflicting reports demonstrating that ROS can either activate[46-48] or inactivate STAT3.[49-51] The early activation of STAT3 followed by late, abrupt inactivation in Dox-treated DLBCL cells is consistent with a model in which the initial rise in ROS levels activates STAT3, possibly through tyrosine kinases such as Syk,[48] culminating in SOD2

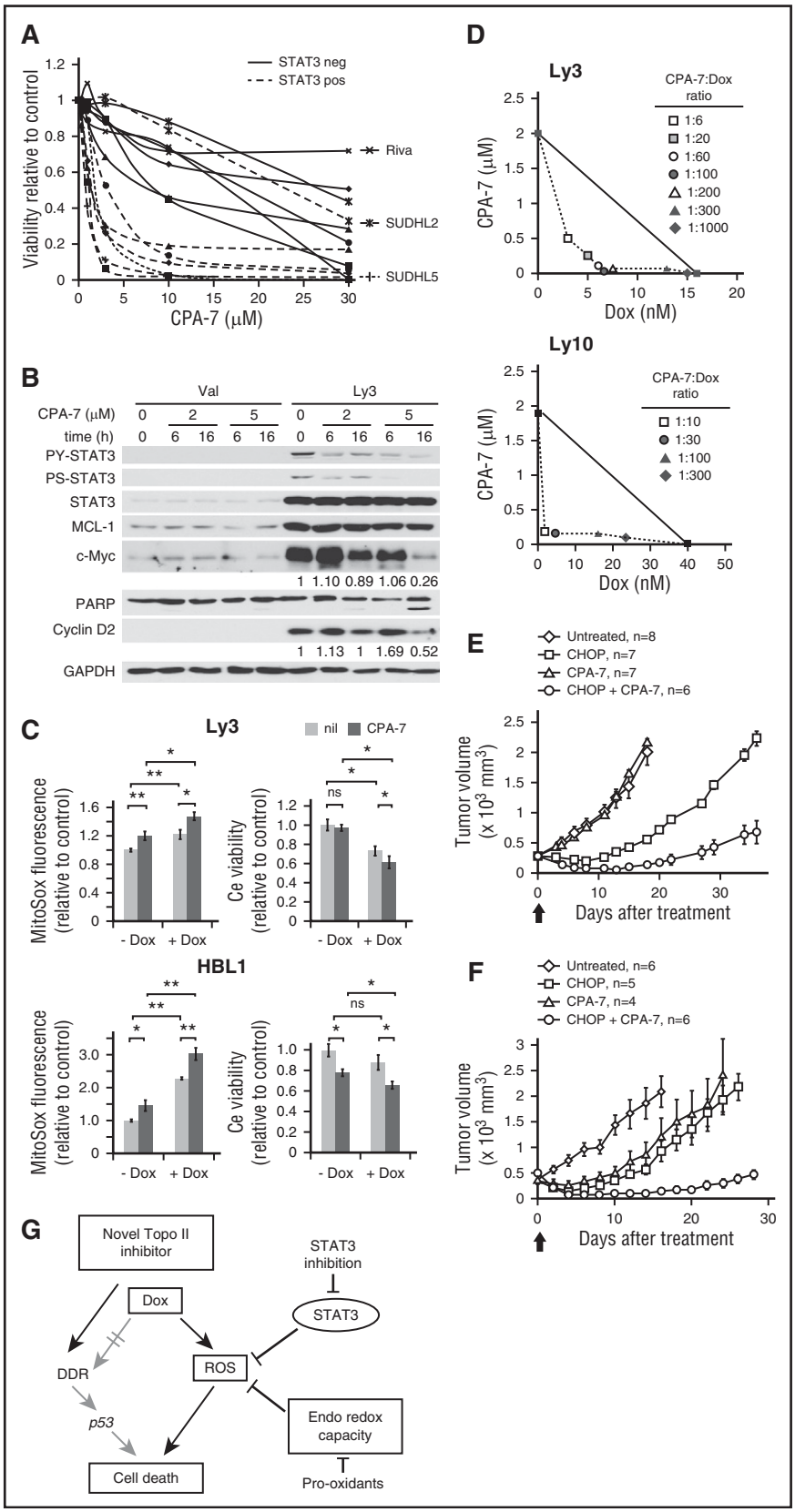

Figure 6. The STAT3 inhibitor, CPA-7, can synergize with Dox to kill ABC-DLBCL cells both in vitro and in vivo. (A) Toxicity of CPA-7 in 7 GCB and 7 ABC cell lines was measured by Resazurin-based viability assays. Although most of the ABC lines showed sensitivity to CPA-7 ($IC_{50} \leq 3$ μM), the majority of the GCB lines fell into the resistant group (IC50 > 7 μM). The 3 outliers are individually labeled and discussed in the text. (B) CPA-7 treatment reduced PY-STAT3, c-Myc, and Cyclin D2 in a dose- and time-dependent manner in Ly3 cells. (C) The effect of CPA-7 on basal and Dox-induced ROS and cell viability change. Ly3 and HBL1 cells were pretreated with 0.3 and 1 μM of CPA-7, respectively, for 1 h before exposing to IC_{50} concentrations of Dox for 24 hours. ROS and cell viability measurements were made as in Figure 3. Results shown are mean ± SD and were representative of 3 independent experiments. $^*P < .05$; $^{**}P < .01$, based on 2-tailed Student *t* test was used. ns, not significant. nil, vehicle control. (D) Isobolograms for the combination of Dox with CPA-7 that were isoeffective (IC_{50}) for inhibition of proliferation of Ly3 and Ly10 cells. The diagonal line indicates the zero interaction isobole. Cell viability was measured after drug treatment of 48 hours, using Resazurin-based assays. Results are representative of 3 independent experiments. CPA-7 (3.5 mg/kg) synergized with CHOP to kill established Ly3 (E) and Ly10 (F) tumors in xenograft mouse models. Results presented are mean tumor volumes with error bars indicating standard error of the mean. Compared with CHOP or CPA-7 monotherapy, CHOP/CPA-7 combination showed significant activity ($P < .05$, 2-tailed Student *t* test) at all points after day 6 post the single treatment on day 0, marked by the thick arrow. (G) Model depicting Dox-triggered mechanism of cytotoxicity in ABC-DLBCLs. Specifically, Dox is often inefficient in activating the DDR-p53-cell death axis; instead, it relies on ROS accumulation to cause oxidative cell death, a process that is countered by activated STAT3 and the endogenous antioxidant program. PARP, poly(ADP-ribose) polymerase 1.

upregulation and restoration of redox homeostasis. Yet, as Dox-triggered ROS production exceeds a certain threshold, the transcription activity of STAT3 likely diminishes,[49] contributing to an irreversible loss of redox homeostasis. Additional studies are needed to fully elucidate functional interactions between ROS and STAT3 in lymphoma pathogenesis, as well as therapeutic settings.

Although results from both cell line–based experiments and prognostic analysis support a subtype-specific mechanism of Dox cytotoxicity in DLBCL, this conclusion needs to be validated and extended in future investigations, including subtype-specific clinical trials. In this regard, our findings provide a mechanistic basis for 3 types of new therapeutic approaches for ABC-DLBCL (Figure 6G). First, this study reveals a novel function of STAT3 in these lymphoma cells and further strengthens the rationale for targeting STAT3, a therapeutic strategy we and others have previously proposed.[9-11] Among many small molecule compounds demonstrating STAT3 inhibitory activity, few have entered human trials.[52,53] Another new and conceptually different approach is the antisense-based STAT3 drug that has showed promising single-agent activity in phase 1 trials in patients with refractory lymphoma and non-small cell lung cancer.[54] Because Dox mainly relies on oxidative stress to trigger cytotoxicity in ABC-DLBCLs, the second approach is to combine a prooxidant, such as Imexon,[55] with R-CHOP to weaken the tumor's antioxidant defense. Finally, a structurally distinct Topo II inhibitor may circumvent the shortcoming of Dox in accessing nuclear DNA in ABC-DLBCL cells and generating robust DDR.

Acknowledgments

The authors thank Amit Verma and Xiaohua Wang for helpful comments; Boudewijn Burgering (University Medical Center Utrecht) for providing the *SOD2*-Luc reporter construct; Alan Alfieri for assistance with the IR experiment; Peng Guo for help with the confocal image analysis; and Richard Chahwan, Enguang Bi, and Xiaolei Wei for additional technical assistance. Confocal imaging work and flow cytometry analyses were performed at the Albert Einstein College of Medicine Analytical Imaging and Flow Cytometry facilities, which are supported by a National Cancer Institute Cancer Center Support Grant (P30CA013330). This work was supported by National Institutes of Health Grant R01CA85573 (to B.H.Y.), Leukemia and Lymphoma Society Translational Research Grant 6255 (to B.H.Y.), an American Society of Hematology Bridge Award (B.H.Y.), a pilot grant from the Center for AIDS Research at the Albert Einstein College of Medicine (B.H.Y.), and a research grant from the Chemotherapy Foundation (S.P.). B.H.Y. was a recipient of the Irma T. Hirschl Career Scientist Award. S.P. was a recipient of the Paul Calabresi Career Development Award (K12 CA 132783).

Authorship

Contribution: B.H.Y. conceived the project and designed research. Y.M. performed gene expression and cell phenotype analyses after IR and various drug treatments and did image analysis of Dox subcellular distribution. J.J.Y. and B.B.D. examined CPA-7 response in vitro, and J.J.Y. and Y.M. studied CPA-7 and CHOP interaction in xenograft models. Y.Z. and S.P. contributed to the design of the xenograft experiments. F.Y. assessed effects of Dox-antioxidants combination in vitro. E.E.K. analyzed the phenotype of STAT3C stable cell lines. H.C. performed the initial assessment of Dox-triggered DDR in DLBCL cell lines. B.D. synthesized CPA-7. B.B. correlated SOD2 mRNA expression with STAT3 activation and patient survival, measured expression of OSP16, and supervised all OSP16-based survival analysis. B.B., Z.Y.X.-M., and Z.Y. measured expression of OSP16 and performed survival analysis of cases in GSE31312. K.H.Y. supervised survival analysis of GSE31312 and reviewed the manuscript. B.H.Y. and Y.M. analyzed and interpreted the results, and wrote the manuscript.

Conflict-of-interest disclosure: The authors declare no competing financial interests.

ORCID profiles: B.H.Y., 0000-0002-2281-422X.

Correspondence: B. Hilda Ye, Department of Cell Biology, Albert Einstein College of Medicine, 1300 Morris Park Ave, Bronx, NY 10461; e-mail: hilda.ye@einstein.yu.edu.

References

1. Anderson JR, Armitage JO, Weisenburger DD. Epidemiology of the non-Hodgkin's lymphomas: distributions of the major subtypes differ by geographic locations. Non-Hodgkin's Lymphoma Classification Project. *Ann Oncol*. 1998;9(7):717-720.
2. Lenz G, Staudt LM. Aggressive lymphomas. *N Engl J Med*. 2010;362(15):1417-1429.
3. Klein U, Dalla-Favera R. Germinal centres: role in B-cell physiology and malignancy. *Nat Rev Immunol*. 2008;8(1):22-33.
4. Schneider C, Pasqualucci L, Dalla-Favera R. Molecular pathogenesis of diffuse large B-cell lymphoma. *Semin Diagn Pathol*. 2011;28(2):167-177.
5. Pasqualucci L, Dalla-Favera R. SnapShot: diffuse large B cell lymphoma. *Cancer Cell*. 2014;25(1):132.
6. Lenz G, Davis RE, Ngo VN, et al. Oncogenic CARD11 mutations in human diffuse large B cell lymphoma. *Science*. 2008;319(5870):1676-1679.
7. Compagno M, Lim WK, Grunn A, et al. Mutations of multiple genes cause deregulation of NF-kappaB in diffuse large B-cell lymphoma. *Nature*. 2009;459(7247):717-721.
8. Ngo VN, Young RM, Schmitz R, et al. Oncogenically active MYD88 mutations in human lymphoma. *Nature*. 2011;470(7332):115-119.
9. Ding BB, Yu JJ, Yu RY, et al. Constitutively activated STAT3 promotes cell proliferation and survival in the activated B-cell subtype of diffuse large B-cell lymphomas. *Blood*. 2008;111(3):1515-1523.
10. Lam LT, Wright G, Davis RE, et al. Cooperative signaling through the signal transducer and activator of transcription 3 and nuclear factor-kappaB pathways in subtypes of diffuse large B-cell lymphoma. *Blood*. 2008;111(7):3701-3713.
11. Scuto A, Kujawski M, Kowolik C, et al. STAT3 inhibition is a therapeutic strategy for ABC-like diffuse large B-cell lymphoma. *Cancer Res*. 2011;71(9):3182-3188.
12. Huang X, Meng B, Iqbal J, et al. Activation of the STAT3 signaling pathway is associated with poor survival in diffuse large B-cell lymphoma treated with R-CHOP. *J Clin Oncol*. 2013;31(36):4520-4528.
13. Gutiérrez-García G, Cardesa-Salzmann T, Climent F, et al; Grup per l'Estudi dels Limfomes de Catalunya I Balears (GELCAB). Gene-expression profiling and not immunophenotypic algorithms predicts prognosis in patients with diffuse large B-cell lymphoma treated with immunochemotherapy. *Blood*. 2011;117(18):4836-4843.
14. Nowakowski GS, Czuczman MS. ABC, GCB, and Double-Hit Diffuse Large B-Cell Lymphoma: Does Subtype Make a Difference in Therapy Selection? *Am Soc Clin Oncol Educ Book*. 2015;e449-e457.
15. Dunleavy K, Roschewski M, Wilson WH. Precision treatment of distinct molecular subtypes of diffuse large B-cell lymphoma: ascribing treatment based on the molecular phenotype. *Clin Cancer Res*. 2014;20(20):5182-5193.
16. Rovira J, Valera A, Colomo L, et al. Prognosis of patients with diffuse large B cell lymphoma not reaching complete response or relapsing after frontline chemotherapy or immunochemotherapy. *Ann Hematol*. 2015;94(5):803-812.
17. Young KH, Leroy K, Møller MB, et al. Structural profiles of TP53 gene mutations predict clinical outcome in diffuse large B-cell lymphoma: an international collaborative study. *Blood*. 2008;112(8):3088-3098.
18. Binaschi M, Bigioni M, Cipollone A, et al. Anthracyclines: selected new developments. *Curr Med Chem Anticancer Agents*. 2001;1(2):113-130.
19. Liu LF. DNA topoisomerase poisons as antitumor drugs. *Annu Rev Biochem*. 1989;58:351-375.
20. Bieging KT, Mello SS, Attardi LD. Unravelling mechanisms of p53-mediated tumour suppression. *Nat Rev Cancer*. 2014;14(5):359-370.

21. Bonner WM, Redon CE, Dickey JS, et al. GammaH2AX and cancer. *Nat Rev Cancer*. 2008; 8(12):957-967.
22. Berthiaume JM, Wallace KB. Adriamycin-induced oxidative mitochondrial cardiotoxicity. *Cell Biol Toxicol*. 2007;23(1):15-25.
23. Myers C. The role of iron in doxorubicin-induced cardiomyopathy. *Semin Oncol*. 1998;25(4 Suppl 10): 10-14.
24. Chou TC, Talalay P. Quantitative analysis of dose-effect relationships: the combined effects of multiple drugs or enzyme inhibitors. *Adv Enzyme Regul*. 1984;22:27-55.
25. Mendez LM, Polo JM, Yu JJ, et al. CtBP is an essential corepressor for BCL6 autoregulation. *Mol Cell Biol*. 2008;28(7):2175-2186.
26. Niehans GA, Jaszcz W, Brunetto V, et al. Immunohistochemical identification of P-glycoprotein in previously untreated, diffuse large cell and immunoblastic lymphomas. *Cancer Res*. 1992;52(13):3768-3775.
27. Savatier J, Rharass T, Canal C, et al. Adriamycin dose and time effects on cell cycle, cell death, and reactive oxygen species generation in leukaemia cells. *Leuk Res*. 2012;36(6):791-798.
28. Farrugia MM, Duan LJ, Reis MD, Ngan BY, Berinstein NL. Alterations of the p53 tumor suppressor gene in diffuse large cell lymphomas with translocations of the c-MYC and BCL-2 proto-oncogenes. *Blood*. 1994;83(1):191-198.
29. Horn HF, Vousden KH. Coping with stress: multiple ways to activate p53. *Oncogene*. 2007; 26(9):1306-1316.
30. Lenz G, Wright G, Dave SS, et al; Lymphoma/Leukemia Molecular Profiling Project. Stromal gene signatures in large-B-cell lymphomas. *N Engl J Med*. 2008;359(22):2313-2323.
31. Trachootham D, Alexandre J, Huang P. Targeting cancer cells by ROS-mediated mechanisms: a radical therapeutic approach? *Nat Rev Drug Discov*. 2009;8(7):579-591.
32. Kops GJ, Dansen TB, Polderman PE, et al. Forkhead transcription factor FOXO3a protects quiescent cells from oxidative stress. *Nature*. 2002;419(6904):316-321.
33. Turkson J, Zhang S, Palmer J, et al. Inhibition of constitutive signal transducer and activator of transcription 3 activation by novel platinum complexes with potent antitumor activity. *Mol Cancer Ther*. 2004;3(12):1533-1542.
34. Turkson J, Zhang S, Mora LB, Burns A, Sebti S, Jove R. A novel platinum compound inhibits constitutive Stat3 signaling and induces cell cycle arrest and apoptosis of malignant cells. *J Biol Chem*. 2005;280(38):32979-32988.
35. Kortylewski M, Kujawski M, Wang T, et al. Inhibiting Stat3 signaling in the hematopoietic system elicits multicomponent antitumor immunity. *Nat Med*. 2005;11(12):1314-1321.
36. Assi HH, Paran C, VanderVeen N, et al. Preclinical characterization of signal transducer and activator of transcription 3 small molecule inhibitors for primary and metastatic brain cancer therapy. *J Pharmacol Exp Ther*. 2014;349(3): 458-469.
37. Hochhaus A, Erben P, Ernst T, Mueller MC. Resistance to targeted therapy in chronic myelogenous leukemia. *Semin Hematol*. 2007; 44(1 Suppl 1):S15-S24.
38. Wilson WH. Treatment strategies for aggressive lymphomas: what works? *Hematology Am Soc Hematol Educ Program*. 2013;2013:584-590.
39. Jung K, Reszka R. Mitochondria as subcellular targets for clinically useful anthracyclines. *Adv Drug Deliv Rev*. 2001;49(1-2):87-105.
40. Hindenburg AA, Gervasoni JE Jr, Krishna S, et al. Intracellular distribution and pharmacokinetics of daunorubicin in anthracycline-sensitive and -resistant HL-60 cells. *Cancer Res*. 1989;49(16): 4607-4614.
41. Weaver JL, Pine PS, Aszalos A, et al. Laser scanning and confocal microscopy of daunorubicin, doxorubicin, and rhodamine 123 in multidrug-resistant cells. *Exp Cell Res*. 1991; 196(2):323-329.
42. Altan N, Chen Y, Schindler M, Simon SM. Defective acidification in human breast tumor cells and implications for chemotherapy. *J Exp Med*. 1998;187(10):1583-1598.
43. Pasqualucci L, Trifonov V, Fabbri G, et al. Analysis of the coding genome of diffuse large B-cell lymphoma. *Nat Genet*. 2011;43(9):830-837.
44. Yu H, Pardoll D, Jove R. STATs in cancer inflammation and immunity: a leading role for STAT3. *Nat Rev Cancer*. 2009;9(11):798-809.
45. Camporeale A, Demaria M, Monteleone E, et al. STAT3 Activities and Energy Metabolism: Dangerous Liaisons. *Cancers (Basel)*. 2014;6(3): 1579-1596.
46. Yoon S, Woo SU, Kang JH, et al. STAT3 transcriptional factor activated by reactive oxygen species induces IL6 in starvation-induced autophagy of cancer cells. *Autophagy*. 2010;6(8): 1125-1138.
47. Simon AR, Rai U, Fanburg BL, Cochran BH. Activation of the JAK-STAT pathway by reactive oxygen species. *Am J Physiol*. 1998;275(6 Pt 1): C1640-C1652.
48. Uckun FM, Qazi S, Ma H, Tuel-Ahlgren L, Ozer Z. STAT3 is a substrate of SYK tyrosine kinase in B-lineage leukemia/lymphoma cells exposed to oxidative stress. *Proc Natl Acad Sci USA*. 2010; 107(7):2902-2907.
49. Li L, Cheung SH, Evans EL, Shaw PE. Modulation of gene expression and tumor cell growth by redox modification of STAT3. *Cancer Res*. 2010; 70(20):8222-8232.
50. Kaur N, Lu B, Monroe RK, Ward SM, Halvorsen SW. Inducers of oxidative stress block ciliary neurotrophic factor activation of Jak/STAT signaling in neurons. *J Neurochem*. 2005;92(6): 1521-1530.
51. Li L, Shaw PEA. A STAT3 dimer formed by inter-chain disulphide bridging during oxidative stress. *Biochem Biophys Res Commun*. 2004;322(3): 1005-1011.
52. Sen M, Thomas SM, Kim S, et al. First-in-human trial of a STAT3 decoy oligonucleotide in head and neck tumors: implications for cancer therapy. *Cancer Discov*. 2012;2(8):694-705.
53. Furqan M, Akinleye A, Mukhi N, Mittal V, Chen Y, Liu D. STAT inhibitors for cancer therapy. *J Hematol Oncol*. 2013;6:90.
54. Hong D, Kurzrock R, Kim Y, et al. AZD9150, a next-generation antisense oligonucleotide inhibitor of STAT3 with early evidence of clinical activity in lymphoma and lung cancer. *Sci Transl Med*. 2015;7(314):314ra185.
55. Barr PM, Miller TP, Friedberg JW, et al. Phase 2 study of imexon, a prooxidant molecule, in relapsed and refractory B-cell non-Hodgkin lymphoma. *Blood*. 2014;124(8):1259-1265.
56. Chan DW, Son SC, Block W, et al. Purification and characterization of ATM from human placenta. A manganese-dependent, wortmannin-sensitive serine/threonine protein kinase. *J Biol Chem*. 2000;275(11):7803-7810.